

## Supporting Information for “Episodic Southern Ocean heat loss and its mixed layer impacts revealed by the furthest south multi-year surface flux mooring”

S. B. Ogle<sup>1</sup>, V. Tamsitt<sup>1</sup>, S. A. Josey<sup>2</sup>, S. T. Gille<sup>1</sup>, I. Cerovečki<sup>1</sup>, L. D. Talley<sup>1</sup> and R. A. Weller<sup>3</sup>

<sup>1</sup>Scripps Institution of Oceanography, La Jolla, California 92093, USA

<sup>2</sup>National Oceanography Centre, Southampton, UK

<sup>3</sup>Woods Hole Oceanographic Institution, Woods Hole, MA, USA

### Contents

1. Text S1 to S 4
2. Figures S1 to S 5
3. Tables S1 to S2

### Introduction

This Supporting Information comprises four sections of text, five figures, and two tables. In Text S1, the Ocean Observatories Initiative (OOI) mooring flux data processing and quality control are described in detail. In Text S2, we discuss the mixed layer depth calculations from mooring CTD data, in Text S3, we explain the combined mooring and reanalysis estimate of the annual mean net heat flux and heat flux components, and in Text S4 we describe the probability density of heat flux events.

### Text S1. Mooring data processing

The entire mooring array is designed to be replaced annually, meaning that any instrument biases or calibration drifts on the mooring array will change with each redeployment. Intercomparison of ship-based and overlapping surface mooring observations during the deployment and recovery cruises show reasonable agreement between the ship and surface mooring air-sea flux data [Weller *et al.*, 2015; Bigorre *et al.*, 2017; Curry *et al.*, 2017].

Sensors from METBK11 were not used in the first deployment, since they were damaged during the 2015 RV Atlantis deployment resulting in flawed data. For much of the 2015 austral winter the Surface Apex Mooring had insufficient power to operate, but we have some data from the recovered profiler mooring and flanking moorings during this time. Data from sensor package METBK11  $Q_{SW}$  were flawed for the majority of the second deployment, likely resulting from unknown instrument damage several weeks after deployment. Therefore, sensor package METBK12 was used during the first and second deployments. In the third deployment, sensor package METBK11 was used since it had more coverage than sensor package METBK12, and both agreed well at times of dual reporting. We note that for the third deployment after May 2017, processed relative wind speed and net longwave, latent, and sensible heat flux components that rely on relative wind speed are currently unavailable from OOI. Comparison of the duplicate sensors (mean and RMS differences) for each flux component for all three deployments are shown in Table S1.

With the exception of  $Q_{SW}$  and SST, all of the variables have undergone automatic OOI Quality Control (QC) algorithms (Global Range test, Spike test, and Trend test). The OOI Global Range test and Trend test falsely flagged some  $Q_{SW}$  and SST data, so we did

---

Corresponding author: V. Tamsitt, [veronica.tamsitt@gmail.com](mailto:veronica.tamsitt@gmail.com)

not apply these tests to  $Q_{SW}$  and SST. We applied our own additional manual quality control steps to remove outliers, negative  $Q_{SW}$  values, repeating values, and zero wind values.

### **Text S2. Mixed layer depth calculations**

Mixed layer depths (MLDs) are calculated from Argo float profiles using the density threshold method of *Montégut et al.* [2004], with a density threshold of  $0.03 \text{ kg m}^{-3}$  and a reference depth of 10 m. However, the floats used are not located exactly at the mooring (they are within  $52.5\text{-}57.5^\circ\text{S}$  and  $85\text{-}95^\circ\text{W}$ ; see Figure S2); thus, we also estimate mixed layer depths at the profiler mooring and flanking moorings.

For the profiler mooring, which only profiles below 180 m depth, we reference to the shallowest surface mooring CTD at 12 m depth, when it provides data. When the surface mooring CTD at 12 m does not have data (especially in winter 2015), we use the 30 m CTD from flanking mooring A. Unfortunately, the profiler mooring only has data during the 2016 winter. Since the Argo float MLDs are similar to the profile MLDs in winter 2016, it is reasonable to assume that the Argo float MLDs are somewhat representative of the mooring location.

In addition, we use the discrete CTDs mounted on flanking mooring A (flanking mooring B had less data coverage and a bad salinity sensor so was not used) to identify times when MLDs at flanking mooring A are greater than 250 m. Flanking mooring A has data for most of 2015 and 2016 (except for the end of June 2015 and beginning of July 2015). Outliers were manually removed from the flanking mooring A dataset. The surface mooring CTDs have very limited data for determining MLDs so only the 12 m CTD was used as a MLD reference depth.

Because of the sparse vertical positioning of instruments on the surface and flanking moorings, the MLDs calculated from CTDs (flanking mooring A is the only one shown; see Figures S3 and S4) represent ranges between which the MLD is located. We use a 30 m reference depth for flanking mooring A. In analysis not shown, flanking mooring B shows slightly more MLDs deeper than 250 m in October 2016 than flanking mooring A. Overall, the flanking moorings demonstrate the same interannual variability (deeper MLDs in winter 2015 than 2016), but also show that there is some heterogeneity of MLDs in this region. While there is reasonably good agreement between MLDs calculated from the floats and the profiler mooring, larger discrepancies arise when the float locations deviate further from the mooring location. The deep MLDs identified by the flanking moorings are also consistent with the float and profiler mooring MLDs.

### **Text S3. Episodic heat loss events**

Episodic heat loss events correspond to exceptional negative values of the turbulent heat flux ( $Q_{SH} + Q_{LH}$ ). Figure S1 shows the probability density function of  $Q_{SH} + Q_{LH}$ . The PDF of turbulent heat loss events has a single peak that is skewed negative (negative events are further from the mean than positive events). Although the PDF is not formally Gaussian, as demonstrated by the differences between the red line and black bars, we use the two standard deviation ( $2\sigma$ ) and three standard deviation ( $3\sigma$ ) thresholds to identify turbulent heat loss events in this analysis.

### **Text S4. Annual mean flux estimation**

We use NCEP-NCAR Reanalysis 1 (NCEP1 hereafter, [*Kalnay et al.*, 1996]) estimates of  $Q_{LW}$ ,  $Q_{LH}$ , and  $Q_{SH}$  components in Nov 2015 along with the OOI mooring flux data to estimate the annual mean of each flux component at the OOI surface mooring. NCEP1 individual monthly means for each flux component are regressed onto the corresponding mooring monthly means using all available data from February 2015 through August 2017.

We then apply the regression relationships to the NCEP1 monthly mean values for Nov 2015 in order to generate a combined OOI/NCEP1 estimate of the three missing flux component means for this particular month. The corrections are  $\Delta Q_{LH} = +5$ ,  $\Delta Q_{SH} = -4$ , and  $\Delta Q_{LW} = +25 \text{ W m}^{-2}$ . Any biases arising from the OOI/NCEP1 estimates will have a relatively small effect on the annual mean as they are only applied in one month (for example, a  $20 \text{ W m}^{-2}$  monthly bias has less than  $2 \text{ W m}^{-2}$  impact in the annual mean). Note, if the NCEP correction is applied to all of the available monthly data, the root mean square difference between the mooring data and NCEP-NCAR falls from  $34.8 \text{ W m}^{-2}$  to  $9.4 \text{ W m}^{-2}$  demonstrating the validity of the approach.

## References

- Bigorre, S., V. Tamsitt, M. Horn, J. Kemp, T. Thomas, L. Houghton, M. Ochs, and R. Sanger (2017). Southern Ocean 2 Deployment Cruise Report Ver 1-01, *Ocean Observatories Initiative*, Control Number: 3201-00203, Retrieved from <https://alfresco.oceanobservatories.org/alfresco/faces/jsp/browse/browse.jsp>.
- Carter, B. R., L. D. Talley, and A. G. Dickson (2014), Mixing and remineralization in waters detrained from the surface into Subantarctic Mode Water and Antarctic Intermediate Water in the southeastern Pacific, *Journal of Geophysical Research: Oceans*, 119(6), 4001–4028
- Curry, R., A. Alai, C. Basque, S. Caldwell, B. Guerro, C. Haskins, L. Houghton, J. Kuo, J. Mitchell, W. Ostrom, T. Thomas, G. Yonkoske (2017). Southern Ocean 3 Deployment Cruise Report Ver 1-00, *Ocean Observatories Initiative*, Control Number: 3201-00203, Retrieved from <https://alfresco.oceanobservatories.org/alfresco/faces/jsp/browse/browse.jsp>.
- de Boyer Montégut, C., G. Madec, A. S. Fischer, A. Lazar, and D. Iudicone (2004), Mixed layer depth over the global ocean: An examination of profile data and a profile-based climatology, *J. Geophys. Res.*, 109, C12, doi:10.1029/2004JC002378.
- Holte, J.W., L.D. Talley, T.K. Chereskin, and B.M. Sloyan (2012), The role of air-sea fluxes in Subantarctic Mode Water formation, *Journal of Geophysical Research: Oceans*, 117, C03040.
- Kalnay, E., M. Kanamitsu, R. Kistler, W. Collins, D. Deaven, L. Gandin, M. Iredell, S. Saha, G. White, J. Woollen et al. (1996), *Bulletin of the American meteorological Society*, 77(3), 437–471.
- Marshall, G. and National Center for Atmospheric Research Staff (Eds). Last modified 10 Jun 2016. "The Climate Data Guide: Marshall Southern Annular Mode (SAM) Index (Station-based)." Retrieved from <https://climatedataguide.ucar.edu/climate-data/marshall-southern-annular-mode-sam-index-station-based>.
- Weller, B, D. Gassier, K. Newhall, B. Pietro, D. Wellwood, E. Morris, J. Ryder, G. Chavez, A. Alai, and J. Lund (2015). Southern Ocean 1 Deployment Cruise Report Ver 1-00, *Ocean Observatories Initiative*, Control Number: 3201-00103, Retrieved from <https://alfresco.oceanobservatories.org/alfresco/faces/jsp/browse/browse.jsp>.

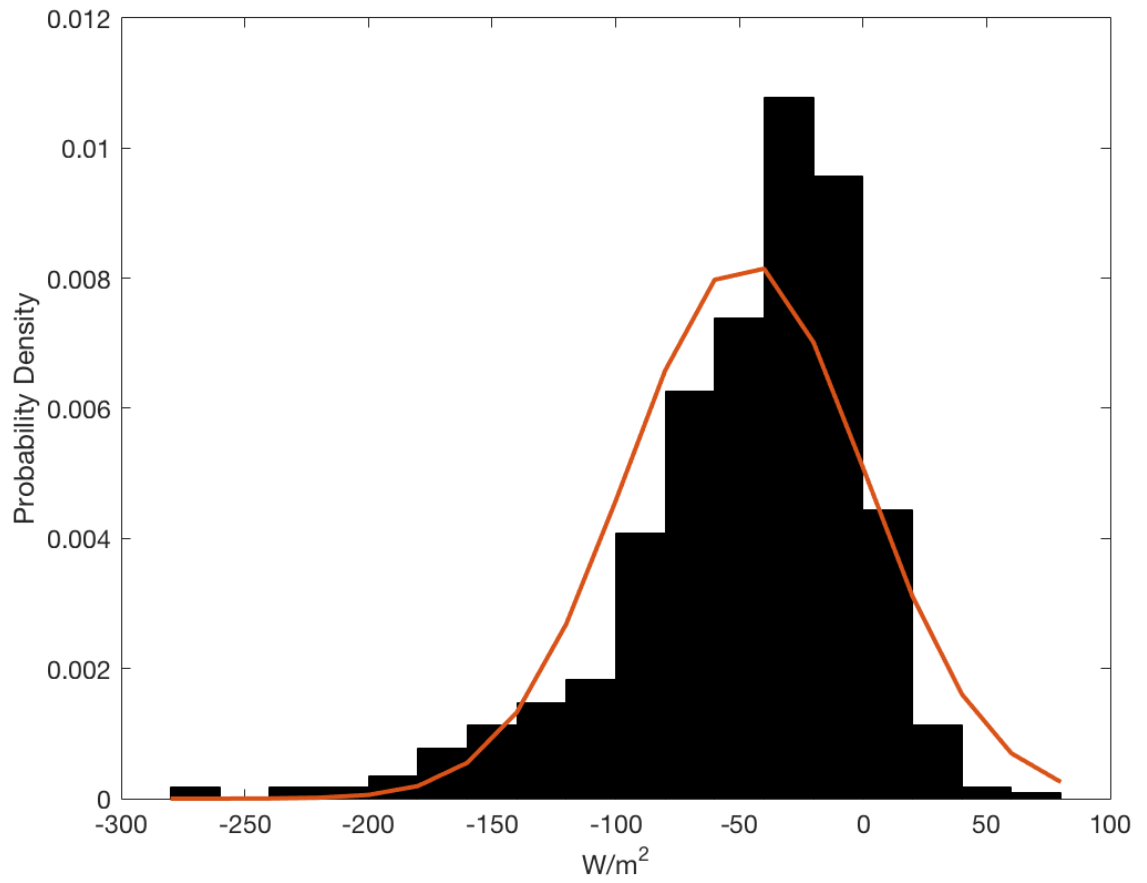


**Figure 1.** Probability density of daily-averaged turbulent air-sea heat fluxes computed from all available mooring data (black bars), with red line indicating best Gaussian fit to this distribution.

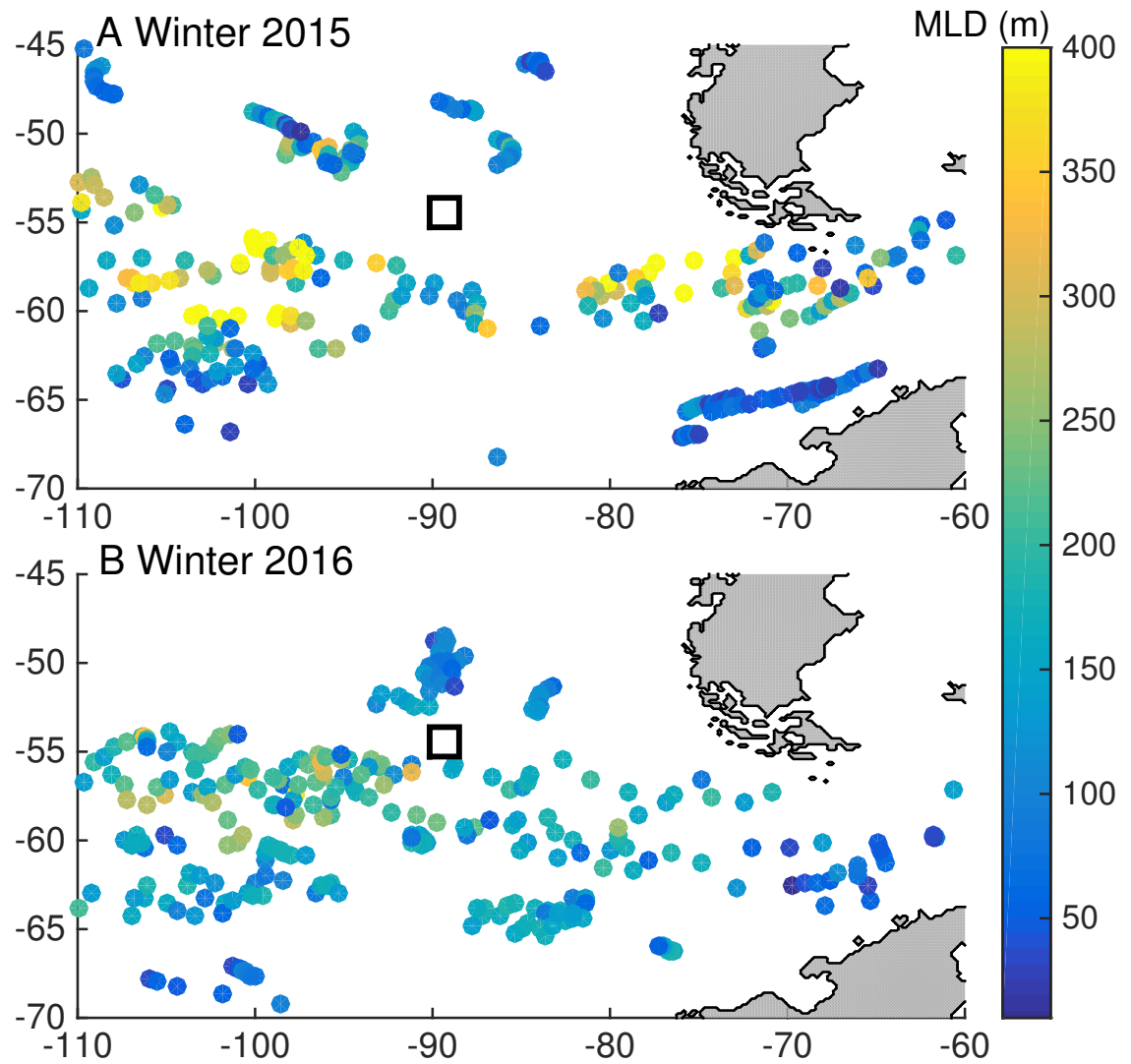


**Figure 2.** Winter (August, September, October) mixed layer depths from Argo float profiles (color) in the Southeast Pacific for a) 2015 and b) 2016. Black squares in each panel indicate the OOI Southern Ocean mooring array location.

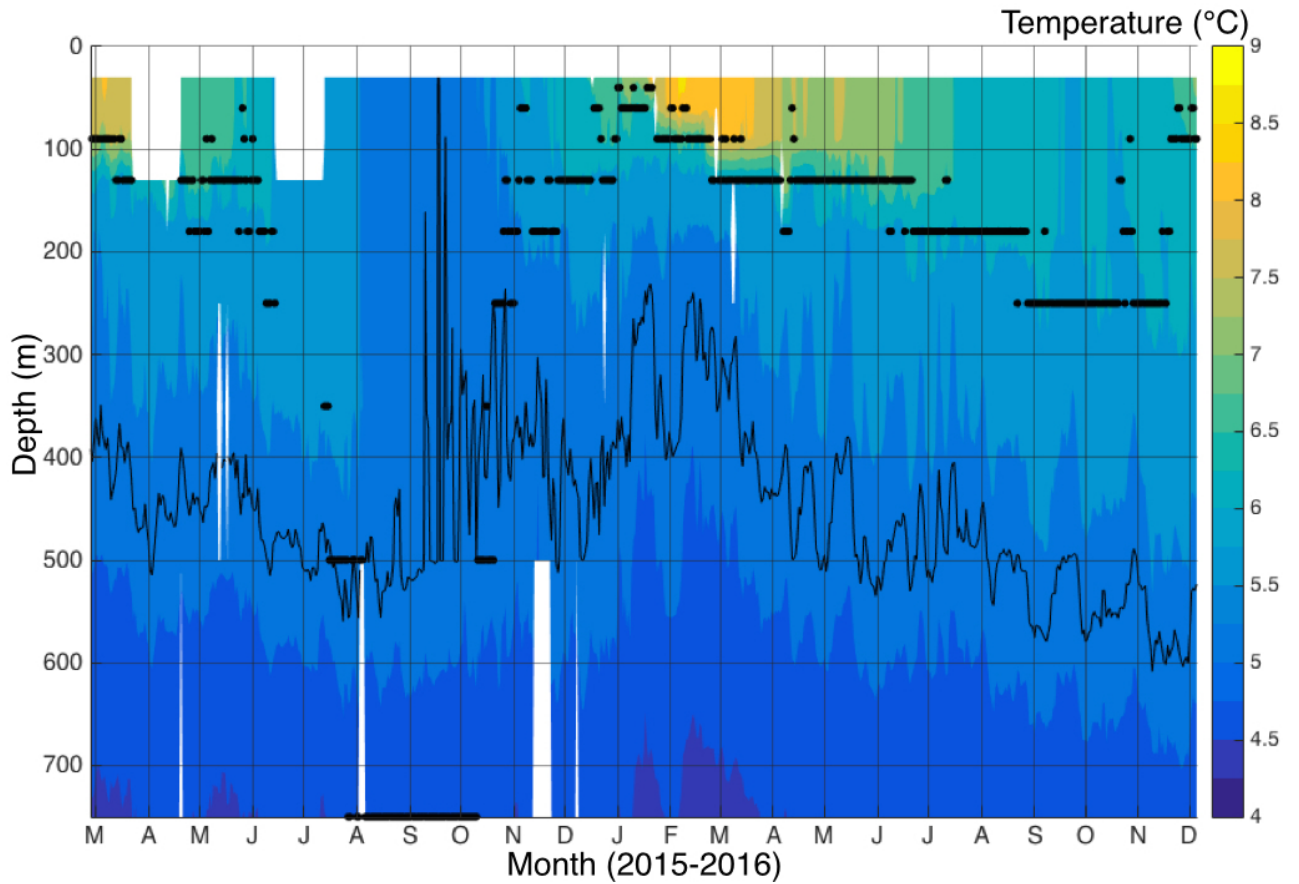


**Figure 3.** Flanking mooring A daily average potential temperature from CTDs (30 m, 40 m, 60 m, 90 m, 130 m, 180 m, 250 m, 350 m, 500 m, and 750 m). The black contour shows when the potential temperature is 5.25°C, the upper limit of Subantarctic Mode Water in this region from *Carter et al.* [2014]. Black dots represent the maximum MLD identified by Flanking mooring A CTDs. For example, a dot at 350 m represents the first time the potential density is  $0.03 \text{ kg m}^{-1}$  different from the 30 m CTD; thus, the MLD would be between 250 m and 350 m.

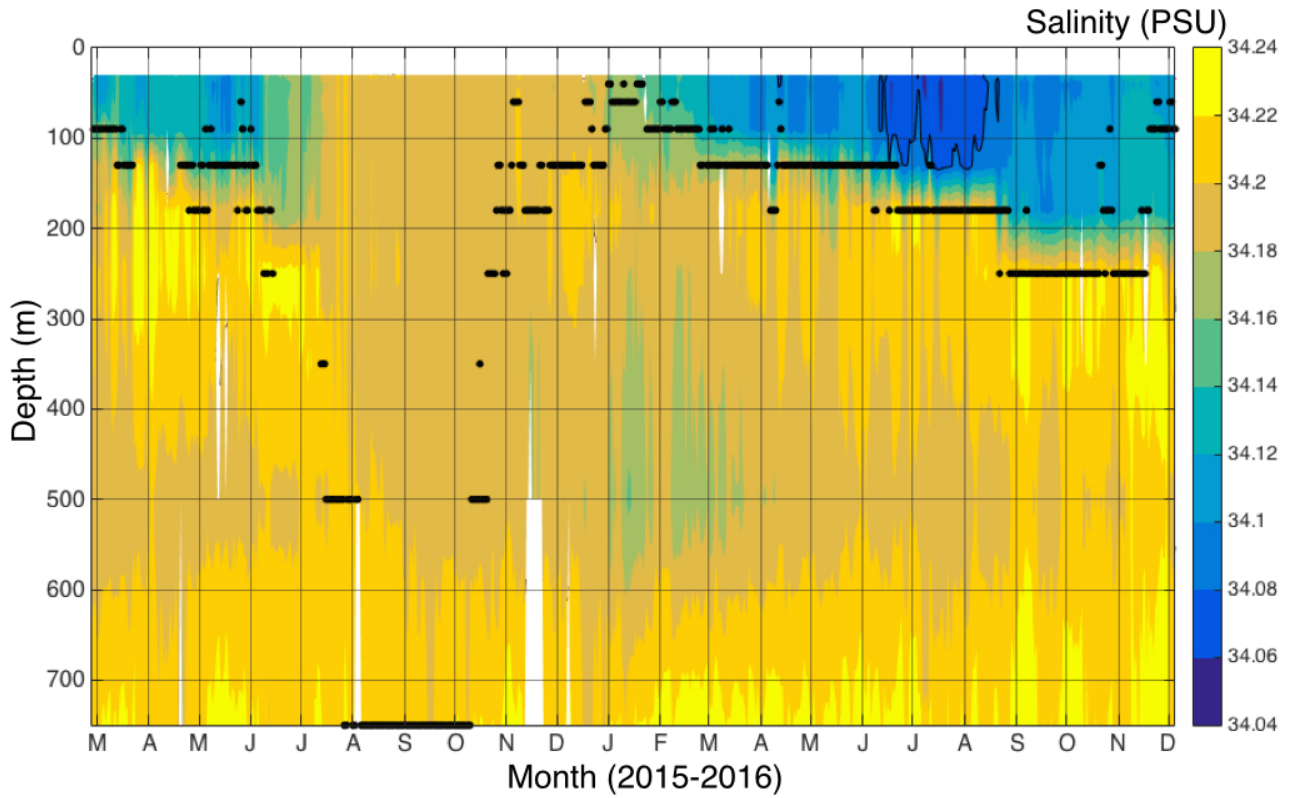


**Figure 4.** Flanking mooring A practical salinity with 34.08 PSU contoured, showing the minimum salinity for SAMW from *Holte et al.* [2012]. Black dots show the maximum MLD from Flanking mooring A (as in Figure S3).

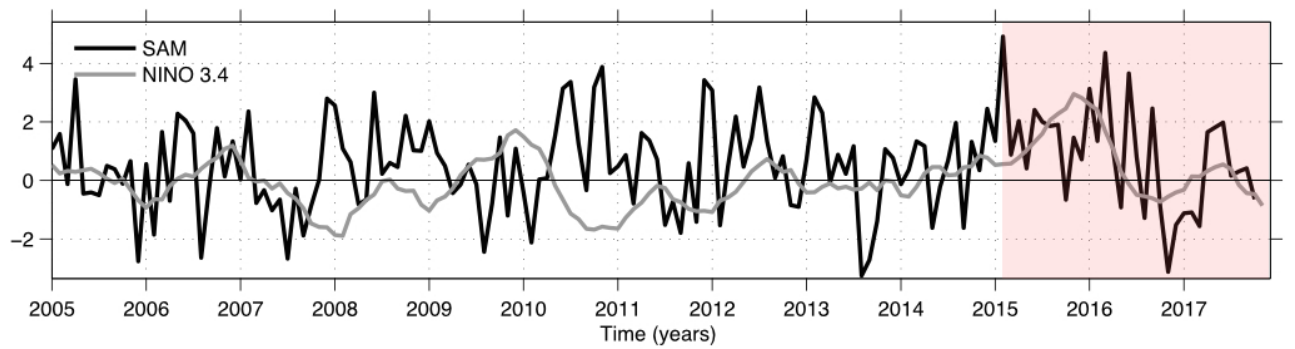


**Figure 5.** The monthly averaged (gray) NINO3.4 anomaly and (black) the Southern Annular Mode (SAM) index from *Marshall and NCAR Staff* [2016].

**Table 1.** Absolute value of mean and RMS differences (in  $\text{W m}^{-2}$ ) between sensor package 11 and 12 for each heat flux component for the first, second, and third deployments of the OOI surface mooring. Mean and RMS differences are not shown in cases where there was very little QC'd data from one sensor and thus the differences may not be robust.

Flux component	Deployment 1	Deployment 2	Deployment 3
$Q_{\text{SW}}$	3.9/26	–	0.1/15
$Q_{\text{LW}}$	3.7/7.1	2.7/4.8	4.9/6.6
$Q_{\text{LH}}$	–	4.2/19.5	0.2/7.6
$Q_{\text{SH}}$	–	1.4/5.4	0.6/2.6

**Table 2.** Characteristics of  $3\text{-}\sigma$  turbulent heat loss events. We list the date, SST, air temperature, relative wind speed, and total turbulent heat flux (THF).

Date	SST ( $^{\circ}\text{C}$ )	Air temp ( $^{\circ}\text{C}$ )	Wind speed ( $\text{m s}^{-1}$ )	THF ( $\text{W m}^{-2}$ )
02-Apr-2015	7.3	4.0	14	-218
12-Apr-2015	7.1	4.1	17	-220
05-Aug-2015	5.4	0.5	14	-261
06-Aug-2015	5.4	-0.9	12	-262
17-Aug-2015	5.3	1.3	13	-226
05-Apr-2016	7.5	3.8	12	-195
15-Apr-2016	6.4	4.5	13	-204